More Intense, More Frequent, and Longer Lasting Heat Waves in the 21st Century

Gerald A. Meehl, *et al.*

Science **305**, 994 (2004);
DOI: 10.1126/science.1098704

13. A. T. Anderson, A. M. Davis, F. Lu, *J. Petrol.* **41**, 449 (2000).
14. M. R. Reid, C. D. Coath, T. M. Harrison, K. D. McKeegan, *Earth Planet. Sci. Lett.* **150**, 27 (1997).
15. C. A. Chesner, *J. Petrol.* **39**, 397 (1998).
16. Materials and analytical methods are available as supporting material on *Science* Online.
17. Model ^{238}U-^{230}Th ages are derived as described in (*14*). See (*34*) for a review of ^{230}Th dating in magmatic systems. The reported ages are taken to be those of crystallization because of the relatively tight packing of ions within allanite and the tetravalent charge of Th [compare (*35*)]. Reequilibration of Th during magmatic residence will be insignificant: Based on the predictive model of Fortier and Giletti (*36*), Th diffusion would only affect ~2 μm in allanite over a period of 100,000 years at the highest reported temperature of the YTT magma (~780°C). Uncertainty in the calculated ages due to possible variation of initial $^{230}Th/^{232}Th$ during magmatic evolution can be evaluated by assuming that observed eruption-age $^{230}Th/^{232}Th$ activity ratio variations of the YTT (0.358 to 0.433) are representative of the initial range of Th-isotope composition. For reported ages <120 ka, the uncertainty in age associated with the initial ratio is within the analytical uncertainty on the ages, except for the youngest allanite domains which could not have grown from melts that had Th isotope compositions significantly different from that of their host. Reported ages that are 120 to 200 ka could be at most a few percent to, for the older of these, as much as 27% older than allowed by the analytical uncertainty. Those few allanites with ages >200 ka could be substantially older. Thus, the age ranges reported here are conservative.
18. J. B. Thomas, R. J. Bodnar, N. Shimizu, C. Chesner, in *Zircon*, J. M. Hanchar, P. W. O. Hoskin, Eds. (Mineralogical Society of America, Washington, DC, 2004), vol. 53, chap. 3.
19. P. L. Roeder, R. F. Emslie, *Contrib. Mineral. Petrol.* **29**, 275 (1970).
20. MnO/MgO in residual melts of silicic magmas typically increases with fractionation of major mafic silicates. La/Nd also increases except when the fractionating assemblage includes sufficient quantities of allanite, chevkinite, and/or monazite that are rich in light rare earth elements (*37*).
21. M. R Reid, in *Treatise on Geochemistry*, H. D. Holland, K. K Turekian, Eds. (Elsevier, Amsterdam, 2003), vol. 3, chap. 3.05.
22. O. Bachmann, G. W. Bergantz, *J. Petrol.*, **45**, 1565 (2004).
23. O. Bachmann, G. W. Bergantz, *Geology* **27**, 447 (2003).
24. B. D. Marsh, M. R. Maxey, *J. Volcanol. Geotherm. Res.* **24**, 95 (1985).
25. V. R. Troll, H. U. Schmincke, *J. Petrol.* **43**, 243 (2002).
26. G. W. Bergantz, *J. Struct. Geol.* **22**, 1297 (2000).
27. S. Couch, R. S. J. Sparks, M. R. Carroll, *Nature* **411**, 1037 (2001).
28. S. Turner, R. George, D. A. Jerram, N. Carpenter, C. Hawkesworth, *Earth Planet. Sci. Lett.* **214**, 279 (2003).
29. M. Nakagawa, K. Wada, T. Thordarson, C. P. Wood, J. A. Gamble, *Bull. Volcanol.* **61**, 15 (1999).
30. D. M. Robinson, C. F. Miller, *Am. Mineral.* **84**, 1346 (1999).
31. C. A. Bachl, C. F. Miller, J. S. Miller, J. E. Faulds, *GSA Bull.* **113**, 1213 (2001).
32. T. H. Druitt, C. R. Bacon, *Trans. R. Soc. Edinburgh Earth Sci.* **79**, 289 (1988).
33. I. N. Bindeman, J. W. Valley, *Geology* **28**, 719 (2000).
34. M. Condomines, P.-J. Gauthier, O. Sigmarsson, in *Uranium-Series Geochemistry*, B. Bourdon, G. M. Henderson, C. C. Lundstrom, S. P. Turner, Eds. (Mineralogical Society of America, Washington, DC, 2003), vol. 52, chap. 4.
35. E. Dowty, *Am. Mineral.* **65**, 174 (1980).
36. S. M. Fortier, B. J. Giletti, *Science* **245**, 1481 (1989).
37. C. F. Miller, D. W. Mittlefehldt, *Geology* **10**, (1982).
38. C. K. Brooks, P. Henderson, J. G. Ronsbo, *Mineral. Mag.* **44**, 157 (1981).
39. G. A. Mahood, W. Hildreth, *Geochim. Cosmochim. Acta* **47**, 11 (1983).
40. J. Blundy, B. Wood, *Nature* **372**, 452 (1994).
41. W. A. Dollase, *Am. Mineral.* **56**, 447 (1971).
42. A. Ewart, W. L. Griffin, *Chem. Geol.* **117**, 251 (1994).
43. C. A. Chesner, A. D. Ettlinger, *Am. Mineral.* **74**, 750 (1989).
44. J. E. Gardner, P. W. Layer, M. J. Rutherford, *Geology* **30**, 347 (2002).

45. We are grateful to C. Chesner for samples; C. Coath, F. Ramos, and F. Kyte for analytical help; and especially J. Simon and G. Bergantz for insightful discussions. Anonymous referees provided very helpful reviews. Funded by NSF grants EAR-9706519 and EAR-0003601. The University of California, Los Angeles (UCLA), ion microprobe is partially subsidized by a grant from the NSF Instrumentations and Facilities Program.

Supporting Online Material
www.sciencemag.org/cgi/content/full/305/5686/991/DC1
Materials and Methods
Tables S1 and S2
Fig. S1
References

19 February 2004; accepted 9 July 2004

More Intense, More Frequent, and Longer Lasting Heat Waves in the 21st Century

Gerald A. Meehl* and Claudia Tebaldi

A global coupled climate model shows that there is a distinct geographic pattern to future changes in heat waves. Model results for areas of Europe and North America, associated with the severe heat waves in Chicago in 1995 and Paris in 2003, show that future heat waves in these areas will become more intense, more frequent, and longer lasting in the second half of the 21st century. Observations and the model show that present-day heat waves over Europe and North America coincide with a specific atmospheric circulation pattern that is intensified by ongoing increases in greenhouse gases, indicating that it will produce more severe heat waves in those regions in the future.

There is no universal definition of a heat wave, but such extreme events associated with particularly hot sustained temperatures have been known to produce notable impacts on human mortality, regional economies, and ecosystems (*1*–*3*). Two well-documented examples are the 1995 Chicago heat wave (*4*) and the Paris heat wave of 2003 (*5*). In each case, severe hot temperatures contributed to human mortality and caused widespread economic impacts, inconvenience, and discomfort.

In a future warmer climate with increased mean temperatures, it seems that heat waves would become more intense, longer lasting, and/or more frequent (*6*, *7*). However, analyses of future changes in other types of extreme events, such as frost days, show that changes are not evenly distributed in space but are characterized instead by particular patterns related to larger scale climate changes (*8*). Here, we examine future behavior of heat waves in a global coupled climate model, the Parallel Climate Model (PCM). This model has a latitude-longitude resolution of about 2.8° in the atmosphere and a latitude-longitude resolution of less than 1° in the ocean, and it contains interacting components of atmosphere, ocean, land surface, and sea ice. The PCM has been used extensively to simulate climate variability and climate change in a variety of applications for 20th- and 21st-century climate (*6*, *8*–*13*). We analyzed a four-member ensemble (i.e., the model was run four times from different initial states and the four members were averaged together to reduce noise) for 20th-century climate and a five-member ensemble for 21st-century climate. The former includes the major observed forcings for the 20th century encompassing greenhouse gases, sulfate aerosols, ozone, volcanic aerosols, and solar variability (*13*). The latter uses a "business-as-usual" scenario, which assumes little in the way of policy intervention to mitigate greenhouse gas emissions in the 21st century (*14*). We define the present-day reference period as 1961 to 1990 for model and observations and the future as the time period from 2080 to 2099.

First, we sought to define a heat wave. Many definitions could apply to heat waves that quantify the duration and/or intensity of either nighttime minima or daytime maxima (*4*, *5*, *15*, *16*). Here, we used two definitions of heat waves; each has been shown to be associated with substantial societal impacts on human health and economies. The first (*4*) evolved from a study of the 1995 Chicago heat wave; it concentrates on the severity of an annual "worst heat event" and suggests that several consecutive nights with no relief from very warm nighttime minimum temperatures may be most important for health impacts. For present-day climate for North America and Europe (Fig. 1), the means of three consecutive warmest nights for observations and the model show good agreement. Heat waves presently are more severe in the southeast United States (large areas greater than 24°C) and less severe in the northwest United States (equally large areas less than 16°C; Fig. 1, A and C). For Europe, there is more of a north-south gradient in both obser-

National Center for Atmospheric Research (NCAR), Post Office Box 3000, Boulder, CO 80307, USA.

*To whom correspondence should be addressed. E-mail: meehl@ncar.ucar.edu

vations and the model (Fig. 1, B and D), with more severe heat waves in the Mediterranean region (most countries bordering the Mediterranean have values greater than 20°C) and less severe heat in northern Europe (many areas less than 16°C).

Future changes of worst 3-day heat waves defined in this way in the model are not uniformly distributed in space but instead show a distinct geographical pattern (Fig. 1, E and F). Though differences are positive in all areas, indicative of the general increase of nighttime minima, heat wave severity increases more in the western and southern United States and in the Mediterranean region, with heat wave severity showing positive anomalies greater than 3°C in those regions. Thus, many of the areas most susceptible to heat waves in the present climate (greatest heat wave severity in Fig. 1, A to D) experience the greatest increase in heat wave severity in the future. But other areas not currently as susceptible, such as northwest North America, France, Germany, and the Balkans, also experience increased heat wave severity in the 21st century in the model.

The second way we chose to define a heat wave is based on the concept of exceeding specific thresholds, thus allowing analyses of heat wave duration and frequency. Three criteria were used to define heat waves in this way, which relied on two location-specific thresholds for maximum temperatures. Threshold 1 (T1) was defined as the 97.5th percentile of the distribution of maximum temperatures in the observations and in the simulated present-day climate (seasonal climatology at the given location), and T2 was defined as the 81st percentile. A heat wave was then defined as the longest period of consecutive days satisfying the following three conditions: (i) The daily maximum temperature must be above T1 for at least 3 days, (ii) the average daily maximum temperature must be above T1 for the entire period, and (iii) the daily maximum temperature must be above T2 for every day of the entire period (*16*).

Because the Chicago heat wave of 1995 and the Paris heat wave of 2003 had particularly severe impacts, we chose grid points from the model that were close to those two locations to illustrate heat wave characteristics. This choice was subjective and illustrative given that there are, of course, other well-known heat waves from other locations. Also, we are not suggesting that a model grid point is similar to a particular weather station; we picked these grid points because they represent heat wave conditions for regions representative of Illinois and France in the model, and therefore they can help identify processes that contribute to changes in heat waves in the future climate in those regions. We chose comparable grid points from the National Centers for Environmental Prediction (NCEP)/NCAR reanalyses that used assimilated observational data (*17*, *18*) for comparison to the model results.

For both the Paris- and Chicago-area grid points for the five-ensemble members, a future increase in heat wave occurrence is predicted (Fig. 2, A and B). For Chicago, the number of present-day heat waves (1961 to 1990) ranges from 1.09 to 2.14 heat waves per year for the four-ensemble members, whereas for future climate, the range shifts to between 1.65 and 2.44. Thus, the ensemble mean heat wave occurrence increases 25% from 1.66 to 2.08 heat waves per year. The current observed value from NCEP for 1961 to 1990 lies within the present-day range from the model with a value of 1.40 events per year. For Paris, the model ranges from 1.18 to 2.17 heat waves per year at present (the value from the NCEP reanalysis lies barely outside this range at 1.10 days), with the future range shifting to between 1.70 and 2.38. Thus, the ensemble mean heat wave occurrence for the Paris grid point increases 31% from 1.64 to 2.15 heat waves per year. Both observed values from NCEP fall well short of the future range from the model, indicative of the shift to more heat waves per year in the future climate.

There is a corresponding increase in duration at both locations (Fig. 2, C and D). For Chicago, present-day average duration of heat waves from the four–model ensemble members ranges from 5.39 to 8.85 days, encompassing the observed value from NCEP at 6.29 days. For Paris, the present-day model range is 8.33 to 12.69 days, with the NCEP observation lying within that range at 8.40 days. For future climate at the Paris grid point, there is a shift to longer lived heat waves with average duration increasing from 11.39 days to 17.04 days. For both of these regions, similar to what was found for the number of heat waves, the corresponding grid point values from the NCEP reanalyses show the duration to be within or very near the range of the present-day model ensemble members but not the future ensemble members, indicative of the

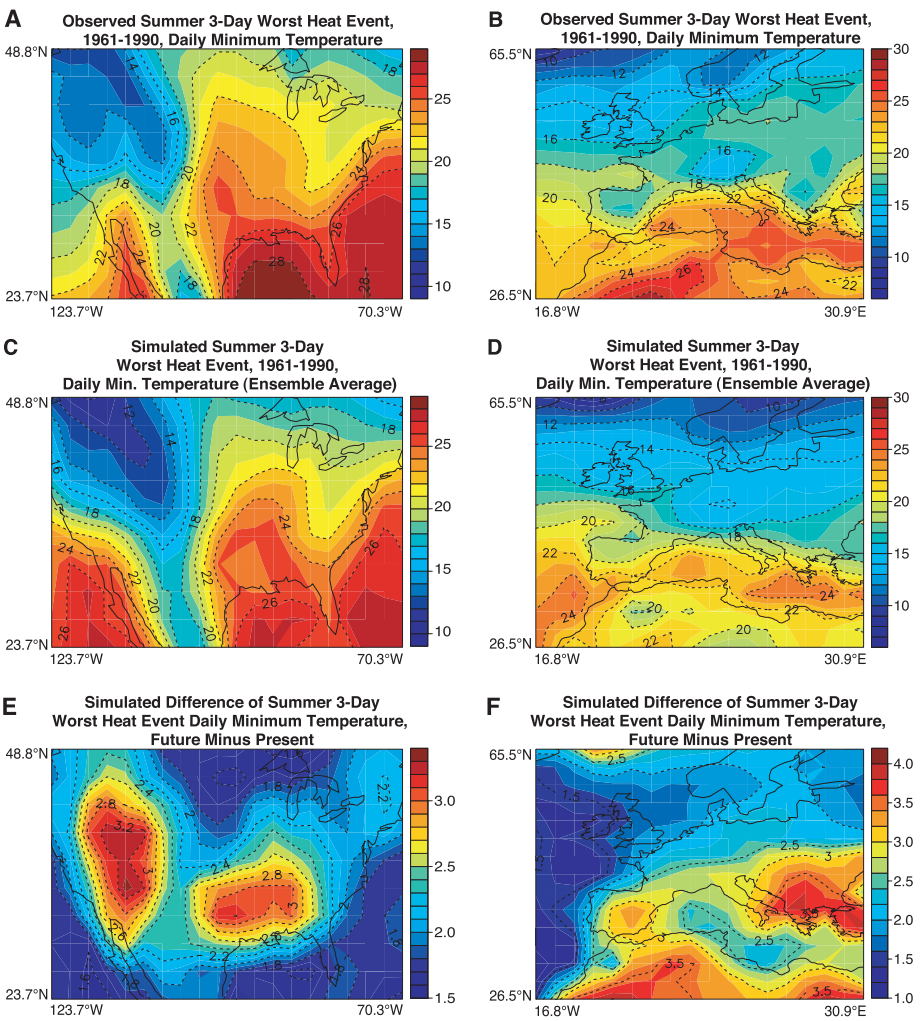

Fig. 1. Heat wave severity as the mean annual 3-day worst (warmest) nighttime minima event (*4*) from NCEP/NCAR reanalyses, 1961 to 1990, for North America (°C) (**A**) and Europe (**B**), and from the model for North America (**C**) and Europe (**D**). The changes of 3-day worst (warmest) nighttime minima event from the model, future (2080 to 2099) minus present (1961 to 1990) for North America (°C) (**E**) and Europe (**F**) are also shown.

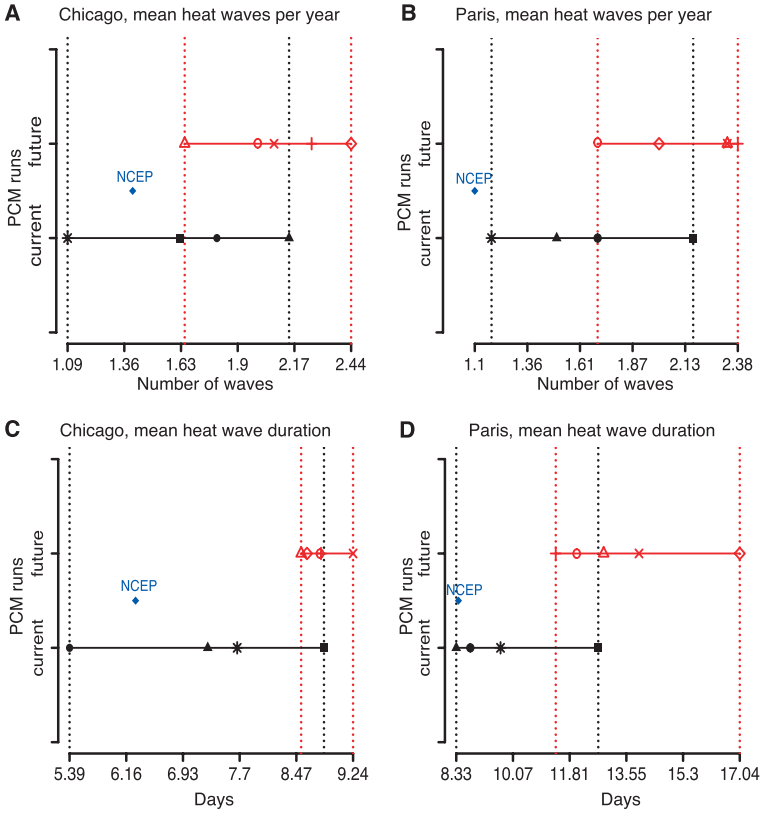

Fig. 2. Based on the threshold definition of heat wave (*16*), mean number of heat waves per year near Chicago (**A**) and Paris (**B**) and mean heat wave duration near Chicago (**C**) and Paris (**D**) are shown. In each panel, the blue diamond marked NCEP indicates the value computed from NCEP/NCAR reanalysis data. The black segment indicates the range of values obtained from the four ensemble members of the present-day (1961 to 1990) model simulation. The red segment indicates the range of values obtained from the five ensemble members of the future (2080 to 2099) model simulation. The single members are marked by individual symbols along the segments. Dotted vertical lines facilitate comparisons of the simulated ranges/observed value.

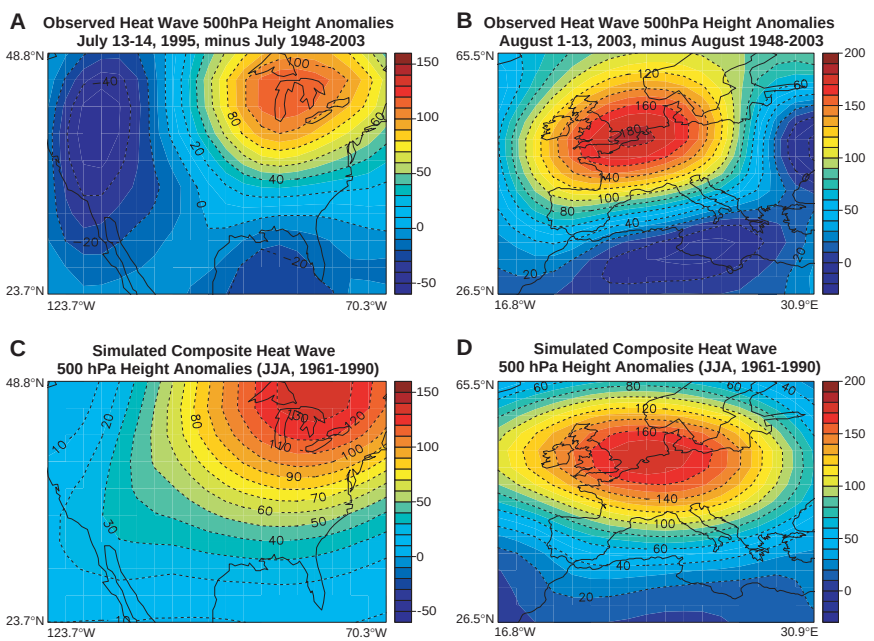

Fig. 3. Height anomalies at 500 hPa (gpm) for the 1995 Chicago heat wave (anomalies for 13 to 14 July 1995 from July 1948 to 2003 as base period), from NCEP/NCAR reanalysis data (**A**) and the 2003 Paris heat wave (anomalies for 1 to 13 August 2003 from August 1948 to 2003 as base period), from NCEP/NCAR reanalysis data (**B**). Also shown are anomalies for events that satisfy the heat wave criteria in the model in present-day climate (1961 to 1990), computed at grid points near Chicago (**C**) and Paris (**D**). In both cases, the base period is summer [June, July, August (JJA)], 1961 to 1990.

shift in the model to more and longer lived heat waves in future climate.

Heat waves are generally associated with specific atmospheric circulation patterns represented by semistationary 500-hPa positive height anomalies that dynamically produce subsidence, clear skies, light winds, warm-air advection, and prolonged hot conditions at the surface (*15*, *19*). This was the case for the 1995 Chicago heat wave and 2003 Paris heat wave (Fig. 3, A and B), for which 500-hPa height anomalies of over +120 geopotential meters (gpm) over Lake Michigan for 13 to 14 July 1995 and +180 gpm over northern France for 1 to 13 August 2003 are significant at greater than the 5% level according to a Student's *t* test. A stratification based on composite present-day heat waves from the model for these two locations over the period of 1961 to 1990 (Fig. 3, C and D) shows comparable amplitudes and patterns, with positive 500-hPa height anomalies in both regions greater than +120 gpm and significance exceeding the 5% level for anomalies of that magnitude.

There is an amplification of the positive 500-hPa height anomalies associated with a given heat wave for Chicago and Paris for future minus present climate (Fig. 4, A and B). Statistically significant (at greater than the 5% level) ensemble mean heat wave 500-hPa differences for Chicago and Paris in the future climate compared with present-day are larger by about 20 gpm in the model (comparing Fig. 4, A and B, with Fig. 3, C and D).

The future modification of heat wave characteristics with a distinct geographical pattern (Fig. 1, E and F) suggests that a change in climate base state from increasing greenhouse gases could influence the pattern of those changes. The mean base state change for future climate shows 500-hPa height anomalies of nearly +55 gpm over the upper Midwest, and about +50 gpm over France for the end of the 21st century (Fig. 4, C and D, all significant above the 5% level). The 500-hPa height increases over the Mediterranean and western and southern United States for future climate are directly associated with more intense heat waves in those regions (Fig. 1, E and F), thus confirming the link between the pattern of increased 500-hPa heights for future minus present-day climate and increased heat wave intensity in the future climate. A comparable pattern is present in an ensemble of seven additional models for North America for future minus present-day climate, with somewhat less agreement over Europe (fig. S1). In that region, there is still the general character of largest positive anomalies over the Mediterranean and southern Europe regions, and smaller positive anomalies to the north (fig. S1), but largest positive values occur near Spain, as opposed to the region near Greece as in our model (Fig. 4D). This also corresponds to a similar pattern for increased standard deviations of both summertime nighttime minimum and daytime

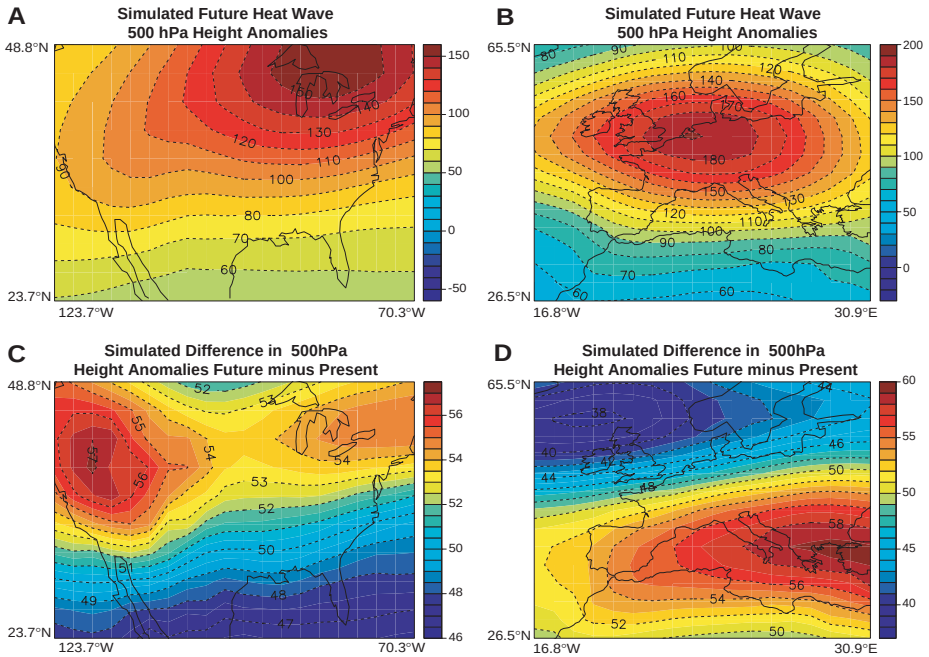

Fig. 4. Height anomalies at 500 hPa (gpm) for events that satisfy the heat wave criteria in the model in future climate (2080 to 2099) for grid points near Chicago (**A**) and Paris (**B**), using the same base period as in Fig. 3, C and D. Also shown are changes (future minus present) in the model's 500-hPa height mean base state, for North America (**C**) and Europe (**D**).

maximum temperatures (fig. S2). This is consistent with a widening of the distribution of temperatures in addition to a shift in the mean (*5*), and suggests that there is an increase in heat wave occurrence beyond that driven by changes in the mean circulation.

The 500-hPa height anomalies are most strongly related to positive warm season precipitation anomalies over the Indian monsoon region and associated positive convective heating anomalies that drive mid-latitude teleconnection patterns (such as those in Fig. 4, C and D) in response to anomalous tropical convective heating in future climate (figs. S3 to S5). Thus, areas already experiencing strong heat waves (e.g., southwest, midwest, and southeast United States and the Mediterranean region) could experience even more intense heat waves in the future. But other areas (e.g., northwest United States, France, Germany, and the Balkans) could see increases of heat wave intensity that could have more serious impacts because these areas are not currently as well adapted to heat waves.

References and Notes

1. C. Parmesan *et al.*, *Bull. Am. Meteorol. Soc.* **81**, 443 (2000).
2. D. R. Easterling *et al.*, *Science* **289**, 2068 (2000).
3. World Health Organization (WHO), "The health impacts of 2003 summer heat waves," WHO Briefing Note for the Delegations of the 53rd session of the WHO Regional Committee for Europe, Vienna, Austria, 8 to 11 September 2003; available at www.euro.who.int/document/Gch/HEAT-WAVES%20RC3.pdf.
4. T. R. Karl *et al.*, *Bull. Am. Meteorol. Soc.* **78**, 1107 (1997).
5. C. Schar *et al.*, *Nature* **427**, 332 (2004).
6. U. Cubasch *et al.*, in *Climate Change 2001: The Scientific Basis. Contribution of Working Group I to the Third Assessment Report of the Intergovernmental Panel on Climate Change*, J. T. Houghton *et al.*, Eds. (Cambridge Univ. Press, Cambridge, 2001), pp. 525–582.
7. T. R. Karl, K. E. Trenberth, *Science* **302**, 1719 (2003).
8. G. A. Meehl *et al.*, *Clim. Dyn.*, in press.
9. W. M. Washington *et al.*, *Clim. Dyn.* **16**, 755 (2000).
10. A. Dai *et al.*, *Geophys. Res. Lett.* **28**, 4511 (2001).
11. G. A. Meehl *et al.*, *J. Clim.* **16**, 426 (2003).
12. B. D. Santer *et al.*, *Science* **301**, 479 (2003).
13. G. A. Meehl *et al.*, *J. Clim.*, in press.
14. A. Dai *et al.*, *J. Climate* **14**, 485 (2001) describes the business-as-usual scenario as similar to the A1B emissions scenario of the Intergovernmental Panel on Climate Change (IPCC) Special Report on Emission Scenarios (SRES) (*20*), with CO_2 rising to about 710 parts per million by volume by 2100, SO_2 emissions declining to less than half the present value by 2100, CH_4 stabilized at 2500 parts per billion by volume in 2100, N_2O as in the IPCC IS92 emissions scenario (*21*), and halocarbons following a preliminary version of the SRES A1B scenario.
15. M. A. Palecki *et al.*, *Bull. Am. Meteorol. Soc.* **82**, 1353 (2001).
16. R. Huth *et al.*, *Clim. Change* **46**, 29 (2000).
17. E. Kalnay *et al.*, *Bull. Am. Meteorol. Soc.* **77**, 437 (1996).
18. Archived observations from surface weather stations, weather balloons, satellites, and other sources are interpolated to a regular grid in a weather forecast model, and the model is run at regular intervals over past time periods to produce a dynamically consistent time-evolving representation of the observed historical climate state.
19. K. E. Kunkel *et al.*, *Bull. Am. Meteorol. Soc.* **77**, 1507 (1996).
20. N. Nakicenovic *et al.*, *IPCC Special Report on Emission Scenarios* (Cambridge Univ. Press, Cambridge, 2000).
21. J. Legget *et al.*, *Climate Change 1992: The Supplementary Report to the IPCC Scientific Assessment* (Cambridge Univ. Press, New York, 1992), pp. 69–75.

22. We thank D. Nychka for discussions; G. Branstator for the convective heating anomaly results; and L. Buja, J. Arblaster, and G. Strand for assistance on the CMIP2+ results from the Coupled Model Intercomparison Project, phase 2 plus (www-pcmdi.llrl.gov/cmip). This work was supported in part by the Weather and Climate Impact Assessment Initiative at the National Center for Atmospheric Research. A portion of this study was also supported by the Office of Biological and Environmental Research, U.S. Department of Energy, as part of its Climate Change Prediction Program, and the National Center for Atmospheric Research. The National Center for Atmospheric Research is sponsored by NSF.

Supporting Online Material
www.sciencemag.org/cgi/content/full/305/5686/994/DC1
Figs. S1 to S5
References

2 April 2004; accepted 9 July 2004

Discovery of Symbiotic Nitrogen-Fixing Cyanobacteria in Corals

Michael P. Lesser,[1]* Charles H. Mazel,[2] Maxim Y. Gorbunov,[3] Paul G. Falkowski[3,4]

Colonies of the Caribbean coral *Montastraea cavernosa* exhibit a solar-stimulated orange-red fluorescence that is spectrally similar to a variety of fluorescent proteins expressed by corals. The source of this fluorescence is phycoerythrin in unicellular, nonheterocystis, symbiotic cyanobacteria within the host cells of the coral. The cyanobacteria coexist with the symbiotic dinoflagellates (zooxanthellae) of the coral and express the nitrogen-fixing enzyme nitrogenase. The presence of this prokaryotic symbiont in a nitrogen-limited zooxanthellate coral suggests that nitrogen fixation may be an important source of this limiting element for the symbiotic association.

The success of scleractinian corals since the Triassic (*1*) has been attributed to the establishment of a mutualistic symbiosis between the cnidarian host and a diverse group of endosymbiotic dinoflagellates (zooxanthellae). Zooxanthellae, which are localized within gastrodermal cells of the cnidarian host, can provide more than